



The behavior of the adsorption of cytochrome C on lipid monolayers: A study by the Langmuir–Blodgett technique and theoretical analysis

Junhua Li, Runguang Sun ^{*}, Changchun Hao ^{*}, Guangxiao He, Lei Zhang, Juan Wang

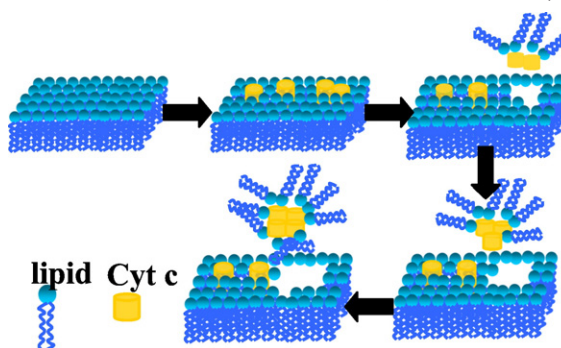
Laboratory of Biophysics and Biomedical Engineering, College of Physics Information Technology, Shaanxi Normal University, Xi'an 710062, China

HIGHLIGHTS

- Theoretical equations are proposed to analyze the behavior of Cyt c on lipid monolayers.
- The quantitative characteristics could be concluded that the different concentrations of Cyt c influence lipid monolayers.
- Theoretical models are introduced that takes into account a phase transition between the LE and LC phase of DPPC.
- The adsorption capacity and conformation reorganization of Cyt c on lipid monolayers are investigated.
- There is a largest adsorption quantity of Cyt c on the lipid monolayers.

GRAPHICAL ABSTRACT

The molecular model of different amounts of Cyt c (0, 2.5, 5, 10, 15 μL , respectively) interaction with lipid monolayer.



ARTICLE INFO

Article history:

Received 31 March 2015

Received in revised form 19 May 2015

Accepted 21 May 2015

Available online 7 June 2015

Keywords:

Cytochrome c

DPPC

DPPE

Monolayer

Atomic force microscopy

Theoretical analysis

ABSTRACT

Cytochrome c (Cyt c) is an essential component of the inner mitochondrial respiratory chain because of its function of transferring electrons. The feature is closely related to the interaction between Cyt c and membrane lipids. We used Langmuir–Blodgett monolayer technique combined with AFM to study the interaction of Cyt c with lipid monolayers at air–buffer interface. In our work, by comparing the mixed Cyt c–anionic (DPPS) and Cyt c–zwitterionic (DPPC/DPPE) monolayers, the adsorption capacity of Cyt c on lipid monolayers is $\text{DPPS} > \text{DPPE} > \text{DPPC}$, which is attributed to their different headgroup structures. π –A isothermal data show that Cyt c ($v = 2.5 \mu\text{L}$) molecules are at maximum adsorption quantity on lipid monolayer. Moreover, Cyt c molecules would form aggregations and drag some lipids with them into subphase if the protein exceeds the maximum adsorption quantity. π –T curve indicates that it takes more time for Cyt c molecular conformation to rearrange on DPPE monolayer than on DPPC. The compressibility study reveals that the adsorption or intermolecular aggregation of Cyt c molecules on lipid monolayer will change the membrane fluidization. In order to quantitatively estimate Cyt c molecular adsorption properties on lipid monolayers, we fit the experimental isotherm with a simple surface state equation. A theoretical model is also introduced to analyze the liquid expanded (LE) to liquid condensed (LC) phase transition of DPPC monolayer. The results of theoretical analysis are in good agreement with the experiment.

© 2015 Elsevier B.V. All rights reserved.

^{*} Corresponding authors.

E-mail addresses: biophymed@snnu.edu.cn (R. Sun), haochangchun@snnu.edu.cn (C. Hao).

1. Introduction

Cytochrome c (Cyt c) is a water soluble metal heme protein, which is widely existed in the inner mitochondrial membrane [1]. It is a relatively small protein (MW = 12000) with a roughly spherical shape of 3.5 nm diameter [2]. Cyt c plays a significant role in the inner mitochondrial respiratory chain because it transfers electrons between the Cyt c reductase and Cyt c oxidase by changing the valence state of the heme iron [1,3–5]. Certainly, the behavior of transferring electrons could promote the combination of hydrogen and oxygen, strengthen oxidation reaction and cell metabolism. In recent years, Cyt c can also be used to study some diseases such as apoptosis and anti-oxidant [6–9]. Numerous researches have been published on Cyt c's structural, physiological and physiochemical properties, and potential applications [10]. Especially, the process and mechanism of Cyt c transferring electrons have been extensively investigated [2,10]. The feature of transferring electrons is closely related to the interaction of Cyt c with membrane lipids [2,11–13]. Moreover, the interaction plays an essential role in determining the conformation of Cyt c, its mitochondrial bilayers location and orientation of heme groups [14–16]. Monolayers play a crucial role in organic electronic devices, since most of the behavior of the transferring electrons occurs on the surface of different functional layers [17].

Phosphatidylcholine (PC) and phosphatidylethanolamine (PE) lipids are relatively abundant lipids in the mitochondrial membranes [18]. Therefore, studying the interaction of Cyt c with DPPC/DPPE has an important biological significance. Langmuir monolayers have been extensively used as model system to mimic natural membrane and to study the thermodynamic behavior of lipid membrane [19–22]. In the present work, there are extensive investigations on the mechanisms of Cyt c association with lipids, but a lot of features of the binding process remain unclear. In particular, the knowledge of the factors controlling the process and protein molecular quantitative characteristics has not yet been explicitly presented [23]. In this paper, the behavior of different concentrations of Cyt c associated with DPPC and DPPE at the air–buffer interface has been studied by surface pressure (π)–time (T), surface pressure (π)–area (A) isotherms as well as the surface compressibility. Moreover, to illustrate the adsorption of Cyt c on lipid monolayers, the morphology of mixed Cyt c–lipid monolayers was observed with AFM. Finally, we applied the surface state equation and the first order equation to analyze the different behavior of the interaction of Cyt c with DPPC/DPPE.

2. Materials and methods

2.1. Materials

Cytochrome c (Cyt c) from equine heart, which is mainly the oxidized form of the protein, at a purity $\geq 95\%$, was purchased from Sigma Chemical Co. (St. Louis, USA) without further purification. 1,2-dipalmitoyl-sn-Glycero-3-phosphocholine (DPPC), 1,2-dipalmitoyl-sn-glycero-3-Phospho-ethanolamine (DPPE) and 1,2-dipalmitoyl-sn-glycero-3-phospho-L-serine (DPPS) were purchased from Avanti Polar Lipids, Inc. (Alabaster, AL, USA). The concentration of lipids solution (dissolved in a mixing solvent of chloroform-methanol (3:1, v/v)) was 1 mg/mL. In all experiments, the subphase was 50 mM phosphate buffer solution (pH = 7.4). All water used was Milli-Q water (18.2 M Ω cm). Cyt c was dissolved in phosphate buffer solution to a final concentration of 1×10^{-4} M for the following experiments.

2.2. Monolayer experiment: surface pressure–area isotherms and surface pressure–time curves measurements

Surface pressure–area (π –A) isotherms and surface pressure–time (π –T) curves were measured on a KSV Minitrough (KSV Instrument, Helsinki, Finland). The trough's effective length and width are 364 mm and 75 mm respectively. The subphase volume is about 240 mL. The

desired lipid was spread onto the surface of the subphase (including the right amount of Cyt c solution) with a Hamilton microsyringe after cleaning the trough. To allow solvent sufficient evaporation, the spread monolayer waited for about 15 min before compressed the monolayer. Then the monolayer was compressed at the speed of 10 mm/min. Simultaneously, the computer would automatically record surface pressure of the monolayer by the Wilhelmy balance method. Monolayers were transferred onto freshly cleaved mica with the transferring rate of 1 mm/min. Surface pressure–time (π –T) curve experiments, in which the monolayer was compressed to an initial pressure and then the changes in pressure with time was recorded (at constant monolayer area), were carried out. All above measurements were performed at 23 ± 1 °C. Every experimental data was repeated at least three times to show satisfactory reproducibility.

2.3. Imaging monolayer with atomic force microscopy (AFM)

Deposited lipid monolayer on the mica was imaged by SPM-9500-J3 AFM (Shimadzu Instruments Co. Ltd., Japan) operating in the contact mode using a Micro-V-shaped Cantilever probe (Olympus Optical Co. Ltd., Japan) that had a spring constant of 0.06 N/m, a length of 100 μ m, and thickness of 400 nm. All images (512 \times 512 points) in height mode were performed in air at a scan rate of 1 Hz.

2.4. Theoretical basis

Fig. 1 is presented according to the early study by Zeng et al. [24]. The experimental π –A isotherms can be analyzed by a simple surface equation [24]

$$\pi = \frac{ZkT}{A} + \frac{\pi_{\max} - ZkT/A}{1 + \exp\left[2 \times \left(\frac{A - A_{LC}}{A_{LC} - A_t}\right)\right]} \quad (1)$$

where π is surface pressure, A, k and T represent the area of each residue in the monolayer, the Boltzmann constant and the temperature, respectively. π_{\max} is the film surface pressure when the monolayer is under the collapse state. A_{LC} , an instantaneous value, is the corresponding area of the intersection of the linear LC-state part of π –A isotherm with its tangent. A_t is a transition area from LC state to collapse state (Fig. 1). The Eq. (1) can be used not only to describe pure phospholipids or protein monolayer but also to describe the binary mixtures. In the above Eq. (1), the value of Z approximates to 1 if monolayer is pure phospholipid, while for protein molecules, the value of Z follows $Z = 1/N_r$, where N_r is the number of residues of protein molecules. However, Eq. (1) is not applicable for the LE–LC phase transition of DPPC. According to Langmuir's report, it is known that part of the molecules will form molecular groups in the process of the LE–LC phase transition. The liquid expanded phase will gradually transform to the liquid condensed phase

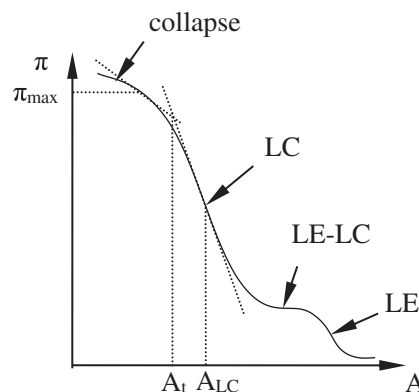


Fig. 1. Typical π –A isotherm of protein or lipid monolayer.

when the molecular groups are further compressed. Considering the process of the LE to LC phase transition, we also introduce the generalized Onnes equation as given in Eq. (2). This equation is not only widely used in practical calculation, but also has a very important theoretical significance.

$$\pi A_m = RT + B_1 \pi + B_2 \pi^2 + B_3 \pi^3 + \dots, \quad (2)$$

or

$$\pi A_m = RT(1 + B'_1 \pi + B'_2 \pi^2 + B'_3 \pi^3 + \dots) \quad (3)$$

where π is surface pressure, A_m is the molecular area/mole. R and T are universal gas constant and the temperature, respectively. B_i or B'_i is the virial coefficient. The virial coefficient is related to the experimental temperature and material properties.

The behavior of protein molecules diffused to the lipid monolayer surface and their conformation rearrangement can be analyzed by the first order Eq. (4) [25].

$$\ln \left(\frac{\pi_e - \pi}{\pi_e - \pi_0} \right) = -\frac{t}{\tau} \quad (4)$$

where τ is relaxation time, π_e , π_0 , π are the surface pressures of interaction between protein and lipid at equilibrium times, $t = 0$, and $t = t$, respectively. The relaxation time τ can be determined by fitting the π - T curves.

3. Results and discussion

3.1. π - A isotherms and theoretical analysis

3.1.1. π - A isotherms

The surface pressure–area (π - A) isotherms of different amounts of Cyt c interaction with DPPC (a), DPPE (b) and DPPS (c) monolayers are shown in Fig. 2. The amounts of Cyt c are 0 μ L, 2.5 μ L, 5 μ L, 10 μ L and 15 μ L, respectively. In Fig. 2(a), pure DPPC monolayer shows the typical phase transition from LE to LC occurring around 3–6 mN/m, which is in good agreement with previously reported values [26]. The surface pressure starts to increase at the area/molecule about 90 \AA^2 . The limiting area/molecule of pure DPPC monolayer is about 45 \AA^2 /molecule, which is estimated by extrapolating the approximate straight part of the π - A isotherm to zero pressure. When the amount of Cyt c is 2.5 μ L, the overall isotherm shows a larger molecular area than pure DPPC due to the adsorption of Cyt c on DPPC monolayer. Meanwhile, a slightly different behavior is observed between mixed Cyt c (2.5 μ L)-DPPC and pure DPPC at lower pressures, which indicates that Cyt c has a greater impact on DPPC monolayer at lower pressures. This may be due to that part of Cyt c molecules adsorb on DPPC monolayer under lower pressures and then they are squeezed into the subphase with DPPC monolayer packed tightly during the sliding barrier

sustained compression. The progressive increase of Cyt c amount, from 5 μ L to 15 μ L, results in a gradual shift of the isotherm toward smaller molecular areas than pure DPPC. The emergence of this phenomenon may be due to Cyt c molecules which form aggregations. These aggregations may drag DPPC molecules with them into the subphase, which is supported by the AFM analysis. We can see that the adsorption quantity of Cyt c on DPPC monolayer has reached a maximum when the amount of Cyt c is 2.5 μ L. Increasing the amount of Cyt c, the mutual repulsion between water molecules and hydrophobic residues of Cyt c molecules is stronger than their attraction, inducing Cyt c molecules aggregated mutually under the van der Waals force. Then these large Cyt c aggregations sink into subphase similar to that reported in the literature [27]. In Fig. 2(a), a well-defined LE–LC transition plateau is observed in all the isotherms.

In case of DPPE monolayer (Fig. 2b), the LE–LC phase transition plateau has not been observed. The mean molecular area/molecule of mixed Cyt c (2.5 μ L, 5 μ L)-DPPE is found to be larger than pure DPPE monolayer. In Fig. 2(a) and (b), our data show that Cyt c molecules have reached a maximum adsorption on DPPC monolayer and DPPE monolayer when the amount of Cyt c is 2.5 μ L. However, a different behavior, the mean molecular area/molecule of mixed Cyt c-DPPC is smaller than pure DPPC but mixed Cyt c-DPPE is larger than pure DPPE, is observed when the amount of Cyt c is 5 μ L. It indicates that Cyt c molecules could be better adsorbed on DPPE monolayer as compared with DPPC monolayer. The smaller headgroup of DPPE in comparison to DPPC may be one deeper reason for this difference [28]. Another reason may be the different shape of their headgroup structures, DPPC is kind of a rodlike molecule while DPPE is the conelike molecule [29].

For auxiliary comparison of the difference in Cyt c adsorption behavior between zwitterionic and negatively charged lipid monolayers, the isotherm of the interaction between Cyt c and DPPS (negatively charged lipid monolayer) was also studied (Fig. 2c). One can see that the surface pressure of pure DPPS starts to increase at the area/molecule of 70 \AA^2 similar to that reported in the literature [30]. The mean molecular area/molecule of mixed Cyt c-DPPS monolayer is larger than pure DPPS monolayer when the amounts of Cyt c are 2.5 μ L, 5 μ L and 10 μ L. By comparing the isotherms of mixed lipid monolayers, the mean molecular area/molecule of mixed Cyt c-DPPC or Cyt c-DPPE is smaller than pure lipid monolayer when the amount of Cyt c is 10 μ L. However, mixed Cyt c-DPPS monolayer shows a larger molecular area than pure DPPS under the same amount of Cyt c.

To better understand the different behavior of Cyt c on lipid monolayers, we calculated the difference value of mean molecular area (ΔA) between mixed Cyt c-lipid monolayers and pure lipid monolayers at the three constant surface pressures of 20 mN/m, 30 mN/m and 50 mN/m (Fig. 3). If $\Delta A > 0$, partial protein molecules adsorb on the lipid monolayers; otherwise, aggregated protein molecules drag lipids with them and sink into subphase. As shown in Fig. 3, the ΔA is much larger for DPPS than for DPPE and DPPC. It indicates that Cyt c is much more readily adsorb on DPPS monolayer. The ΔA of DPPE exhibits a positive value when the amount of Cyt c is 5 μ L, however, the ΔA of DPPC

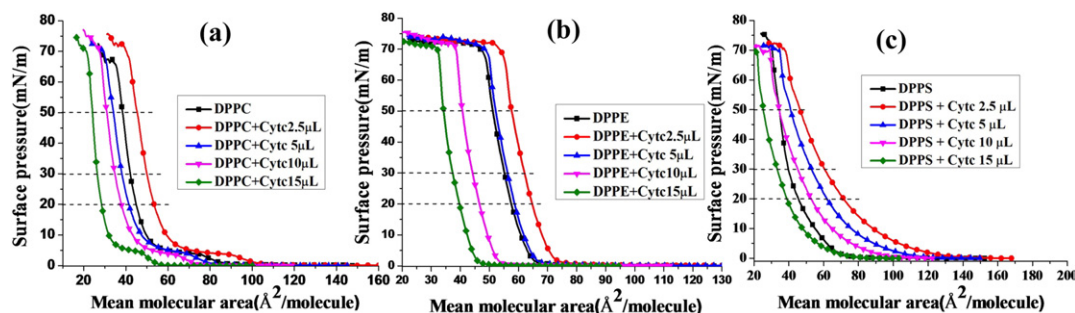


Fig. 2. Surface pressure–area isotherms of different amount of Cyt c interaction with DPPC (a), DPPE (b) and DPPS (c) monolayers on 50 mM phosphate buffer solution (pH = 7.4) subphase at 23 °C. The horizontal dashed line is drawn to better understand Fig. 3.

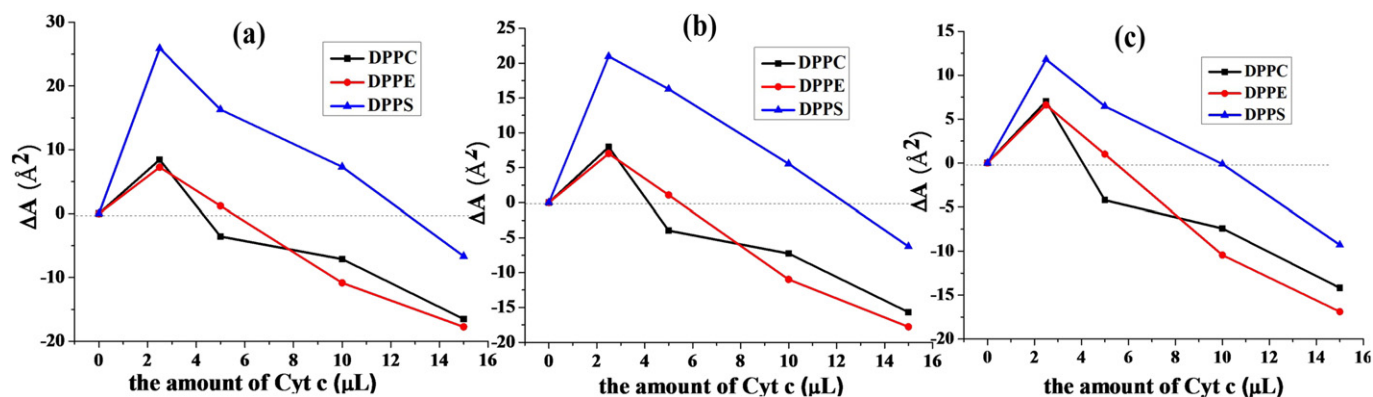


Fig. 3. ΔA (the difference value of mean molecular area between mixed Cyt c-lipid monolayers and pure lipid monolayers) as a function of Cyt c adsorption on lipid monolayers, calculated at different surface pressures: (a) 20 mN/m, (b) 30 mN/m, (c) 50 mN/m.

exhibits a negative value. It indicates that the adsorption capacity of Cyt c on DPPE monolayer is slightly stronger than on DPPC. By comparing the ΔA at the three different constant surface pressures (20 mN/m, 30 mN/m and 50 mN/m) under the same amount of Cyt c, we can see that with the increase of the surface pressure, the ΔA of DPPS monolayer gradually decrease, which indicates that the main driving force of the interaction between Cyt c and DPPS would be electrostatic force under lower pressures. No differences of the ΔA in zwitterionic lipid monolayers (DPPE/DPPE) are observed within the three different surface pressures under the same amount of Cyt c condition.

From the above isotherm results, it is obviously showed that the adsorption capacity of Cyt c on the above-mentioned three lipid monolayers is DPPS > DPPE > DPPC. This may be due to the electrostatic

interaction of the positively charged Cyt c molecules and negatively charged DPPS molecules, which is the major factor in the Cyt c adsorption process.

3.1.2. Theoretical analysis

In order to further investigate the quantitative characteristics of the interaction between Cyt c and DPPC/DPPE monolayer, we focus on the typical experimental data in π -A isotherms (Fig. 2), the amounts of Cyt c are 0 μL , 2.5 μL and 5 μL , which is reasonable because of their sharply different adsorption capacities. These data are analyzed by Eq. (1) and the results are shown in Fig. 4. In Fig. 4(a), the theoretical results are in good agreement with the experimental isotherm data between the LC state and the collapse state. However, these curves don't

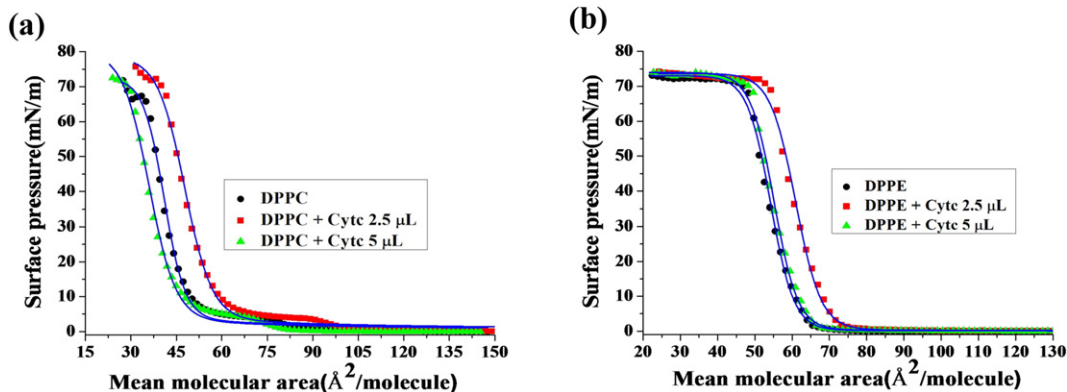


Fig. 4. π -A isotherms of mixed Cyt c-DPPC (a) and Cyt c-DPPE (b) monolayers. The points represent the corresponding experimental data of Fig. 2, theoretical curves (solid lines) calculated from Eq. (1).

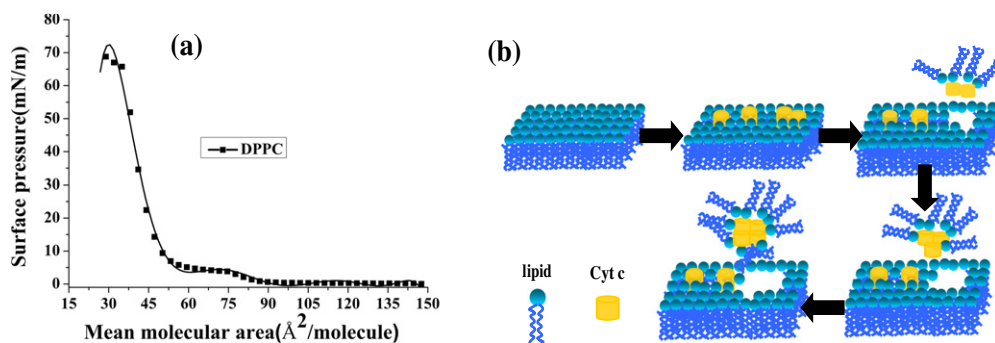


Fig. 5. (a) The points represent the pure DPPC experimental data, theoretical curves (solid lines) calculated by the generalized Onnes equation. (b) The molecular model of different amounts of Cyt c (0, 2.5, 5, 10 and 15 μL , respectively) interaction with lipid monolayer.

Table 1
Parameter values of mixed Cyt c-DPPC in Eq. (1).

The amount of Cyt c	Parameters				
	Π_{\max} (mN/m)	A_{LC}/A_{LC-M} (\AA^2)	A_t/A_{t-M} (\AA^2)	ΔA_{LC} (\AA^2)	R^2
0 μL	72.44	40.89	34.02	6.87	0.994
2.5 μL	78.48	47.67	38.73	8.94	0.995
5 μL	79.96	35.89	27.11	8.78	0.994

Π_{\max} is the film surface pressure when the monolayer is under the collapse state. A_{LC} an instantaneous value, is the corresponding area of the intersection of the linear LC-state part of π -A isotherm with its tangent. A_t is a transition area from LC state to collapse state (Fig. 1). $\Delta A_{LC} = A_{LC} - A_t$. R^2 is the correlation coefficients.

Table 2
Parameter values of mixed Cyt c-DPPE in Eq. (1).

The amount of Cyt c	Parameters				
	Π_{\max} (mN/m)	A_{LC}/A_{LC-M} (\AA^2)	A_t/A_{t-M} (\AA^2)	ΔA_{LC} (\AA^2)	R^2
0 μL	73.02	54.19	47.95	6.24	0.998
2.5 μL	73.65	60.91	54.11	6.80	0.998
5 μL	73.99	55.09	48.56	6.53	0.998

Π_{\max} is the film surface pressure when the monolayer is under the collapse state. A_{LC} an instantaneous value, is the corresponding area of the intersection of the linear LC-state part of π -A isotherm with its tangent. A_t is a transition area from LC state to collapse state (Fig. 1). $\Delta A_{LC} = A_{LC} - A_t$. R^2 is the correlation coefficients.

fit very well with the experimental points at the process of the LE-LC phase transition. To characterize the process of the LE-LC phase transition, the experimental data of DPPC are analyzed by the generalized Onnes equation (Fig. 5a). The Onnes equation can fit the typical LE-LC phase transition and give the values of the different virial coefficients. The related parameters of fitted results are shown in Table 3. It is found that there is no LE-LC phase transition plateau in the theoretical curve when the data are analyzed by Eq. (1) (Fig. 4a). However, the plateau is observed when the data are fitted by the generalized Onnes equation. In our work, all fittings are based on the Origin 8.5.

The related parameters of fitted results by Eq. (1) are showed in Table 1 (Cyt c-DPPC) and Table 2 (Cyt c-DPPE). We focus on four main parameters, Π_{\max} , A_{LC} , A_t , and ΔA_{LC} ($A_{LC} - A_t$). From Tables 1 and 2, we can see that the value of Π_{\max} in mixed monolayers is larger than that in pure phospholipid monolayers. Compared with DPPC or DPPE molecules, Cyt c molecules are much larger and have more complex structures that can't pack tightly even at high pressure, inducing the mixed monolayer, which is not easy to collapse. The theoretical fitted values are in good agreement with experimental data and all the correlation coefficients (R^2) exceed 0.99. The difference value of the A_{LC} between mixed monolayer and pure lipid monolayer is defined as the amount of the Cyt c molecular adsorption on lipid monolayer or surface lipid molecular depletion. It is obviously showed that the difference value of DPPC (6.78 \AA^2) is almost similar to that of DPPE (6.72 \AA^2) when the amount of Cyt c is 2.5 μL . However, when the amount of the Cyt c is 5 μL , the value for DPPC is smaller than DPPE. This study showed that Cyt c molecules are more readily adsorb on the DPPE monolayer than DPPC monolayer under similar condition, which is consistent with the results of previous experimental analysis. What's more, the difference value between A_{LC} and A_t ($\Delta A_{LC} = A_{LC} - A_t$) reflects the

surface compressibility of monolayers (in accordance with the following method).

3.2. Compressibility analysis

To characterize better the surface compressibility of lipid monolayers, the isothermal compressibility C_s is evaluated from π -A isotherms by a physical state equation as follows [31]

$$C_s = -\left(\frac{1}{A}\right)\left(\frac{\partial A}{\partial \pi}\right)_T. \quad (5)$$

Here, A and π represent the mean molecular area/molecule and the surface pressure, respectively. We study the compressibility of Langmuir monolayer to understand the details of phase transition [30] and its stability. In Fig. 6(a), small peak that represents the LE-LC phase transition is observed at the pressure about 3–5 mN/m in all C_s - π curves. When the amount of Cyt c increased from 2.5 μL to 15 μL , there is a relatively large peak at the pressure about 35–50 mN/m. The increase tendency of the peak may be due to the partial Cyt c molecules diffused to the DPPC monolayer surface instantaneously and their conformation rearranged and then formed aggregations. As shown in Fig. 6(a), The C_s of mixed Cyt c (2.5 μL)-DPPC monolayer is smaller than pure DPPC monolayer. This may be due to protein molecule adsorption on DPPC monolayer traducing the membrane fluidization. However, a larger C_s which is more than pure DPPC is presented with increasing amount of Cyt c, from 5 μL to 15 μL , this may be due to the Cyt c molecules which form aggregations and carry some DPPC molecules, eventually sinking into subphase, promoting the membrane fluidization. In terms of mixed Cyt c-DPPE, the C_s of mixed Cyt c (2.5 μL , 5 μL)-DPPE is smaller than pure DPPE, while the value of mixed Cyt c (10 μL , 15 μL)-DPPE is larger than pure DPPE. As shown in Fig. 6(c), the value of mixed Cyt c (10 μL)-DPPS is smaller than pure DPPS, the fluidity of monolayer is reduced by Cyt c adsorption on DPPS monolayer. By comparing the neutral and negatively charged lipid monolayers, the DPPS negatively charged lipid monolayer with a slower fluidity may be caused by the adsorption of Cyt c on the lipid monolayer. Taken together, the smaller C_s and the more adsorption of Cyt c on the lipid surface, induce the tightness of monolayers. When the amount of protein exceeds the maximum adsorption capacity of lipid monolayer, the formed aggregations will carry part of the lipids into subphase, which causes some defects (Fig. 10a, rectangular region) on the lipid monolayer surface, inducing looser monolayers and larger C_s (the result is consistent with previous theoretical analysis of π -A isotherms). The maximum of C_s represents the greatest intermolecular cooperativeness before the full collapse [32], which suggests that the strongest interaction between protein and lipid at the pressure is about 55–65 mN/m.

3.3. π -T curves analysis

The compression of mixed Cyt c (5 μL)-DPPC/DPPE monolayer was interrupted by halting the barrier at the pressure of 20 mN/m, and then π versus time curve was recorded at constant area (Fig. 7). From the experimental data points we can see the π value of mixed Cyt c-DPPC decreasing at about 5.9 mN/m, which is slightly larger than DPPE. The surface pressure begins to decrease until it reaches an equilibrium value at the time of about 2000 s. To analyze the kinetics of

Table 3
The values of the different virial coefficients of pure DPPC calculated by the generalized Onnes equation.

T ($^{\circ}\text{C}$)	Parameters					
	B'_1 ((mN/m) $^{-1}$)	B'_2 ((mN/m) $^{-2}$)	B'_3 ((mN/m) $^{-3}$)	B'_4 ((mN/m) $^{-4}$)	B'_5 ((mN/m) $^{-5}$)	B'_6 ((mN/m) $^{-6}$)
23 $^{\circ}\text{C}$	−1.439	0.174	−8.442 $\times 10^{-3}$	2.195 $\times 10^{-4}$	−3.393 $\times 10^{-6}$	3.216 $\times 10^{-8}$

B'_i is the virial coefficient. The virial coefficient is related to the experimental temperature and material properties.

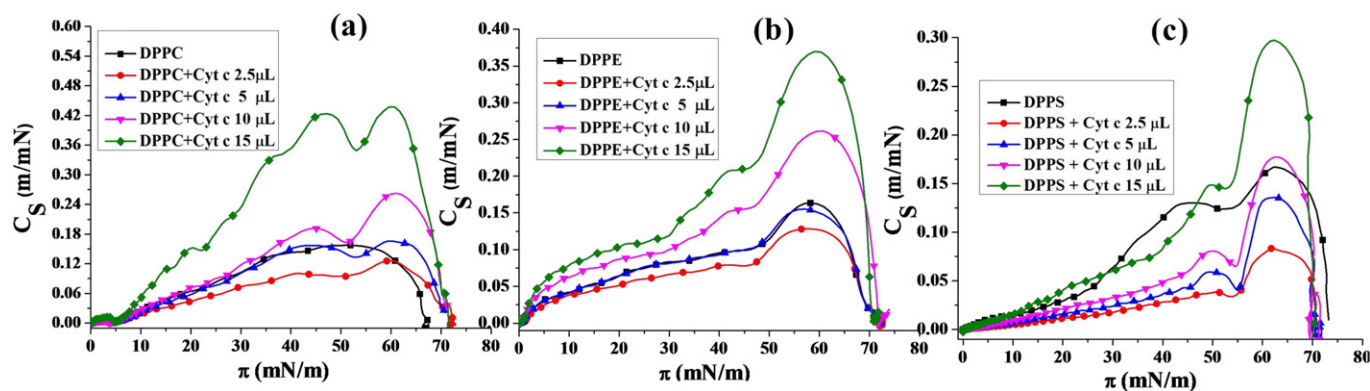


Fig. 6. C_s calculated from π -A isotherm of Fig. 2, mixed Cyt c-DPPC (a), Cyt c-DPPE (b) and Cyt c-DPPS (c).

protein molecules, we focus on the value of parameters π_e , τ , which can be obtained from Eq. (4) by fitting the experimental data points. The equilibrium π_e value of mixed Cyt c-DPPC is about 14.1 mN/m and τ is about 971.9 s, but for mixed Cyt c-DPPE, the $\pi_e = 16.6$ mN/m and $\tau = 1771.7$ s. It is obvious that the experimental data are fitted very well with the theoretical equation. The relaxation time for DPPE is longer than DPPC, which suggests that it takes more time for protein structure to reorganize after binding to DPPE monolayer. The surface pressure decreases rapidly in mixed Cyt c-DPPE and Cyt c-DPPC monolayers when compression is halted, which is attributed to the occurrence of numerous molecular structure changes [33].

3.4. AFM observation

Atomic force microscopy is a new-type and effective method for investigating the lateral domains of monolayer structures. The AFM images of pure DPPE monolayer (Fig. 8a) and DPPC monolayer (Fig. 8b) were transferred on mica at 20 mN/m. As shown in Fig. 8(a), the morphology of pure DPPE monolayer presents “sheet” structures. There are some gaps (isolated dark domains) between these “sheet” structures. The pure DPPC monolayer is uniformly flat with occasional small defects (triangular region in Fig. 8b). In Fig. 9, some white spheres have occurred in the mixed Cyt c-lipid membranes when Cyt c (5 μ L) was added in the subphase, a critical value for the isotherms of DPPC and DPPE monolayer. Therefore, the white spheres are protein molecules. In Fig. 9 (a–c), the morphology of mixed Cyt c-DPPE presents an irregular “sheet” structure and globular domain. It is clearly observed that a small number of protein molecules, rounding a ring structure (elliptic region shown in Fig. 9b and c), attached on the surface of DPPE monolayer (rhombic region showed in Fig. 9b and c). The size of

these protein molecules was measured to be about 39.8 nm in diameter, which indicates that Cyt c molecules are adsorbed in the form of small aggregations, because the diameter of the Cyt c molecular monomer is known to be 3.5 nm [2]. However, most of the proteins (rectangular region shown in Fig. 9b and c) are dispersed homogeneously around DPPE membrane. The dimensions of the globular domains are in the range of 37–71 nm. Thus, the globular domains may be the aggregations of 10 to 20 units of Cyt c molecules.

Compared with mixed Cyt c-DPPE monolayer, as shown in Fig. 9(d–f), the distribution of Cyt c molecules covered on the DPPC monolayer is not uniform and regular. The dimensions of these aggregated Cyt c molecules (white bright spheres) on DPPC monolayer range in size from 68 nm to 532 nm and are much larger than those observed on DPPE monolayer. Thus, Cyt c molecules easily sink into subphase together with some DPPC molecules during the film and continuously compressed to higher surface pressures, which induces smaller mean molecular area/molecule of mixed Cyt c (5 μ L)-DPPC than pure DPPC in π -A isotherm (Fig. 2a). These observations indicate that the interaction of Cyt c with DPPE is stronger than DPPC, which makes most Cyt c molecules evenly embed into the DPPE monolayer with no significant large aggregations. Because of the weakly interaction between Cyt c and DPPC, the increment of intermolecular aggregates of Cyt c molecules may be the main cause for the formation of large aggregations. To further verify that the Cyt c molecules formed aggregations, the AFM images of mixed Cyt c (15 μ L)-DPPE/DPPC monolayer were also studied (Fig. 10). As shown in Fig. 10(a), numerous Cyt c aggregations (white bright spheres) are scattered on DPPE monolayer. Meanwhile, there are some small defects in DPPE monolayer (rectangular region). The size of Cyt c aggregations ranges between approximately 96 nm and 300 nm. These aggregations may be formed by about 28 to 90 units of Cyt c molecules. In Fig. 10(b), the Cyt c aggregations on DPPC monolayer are much larger than on DPPE monolayer. Therefore, the AFM images support the results of π -A isotherm and C_s - π curve studies.

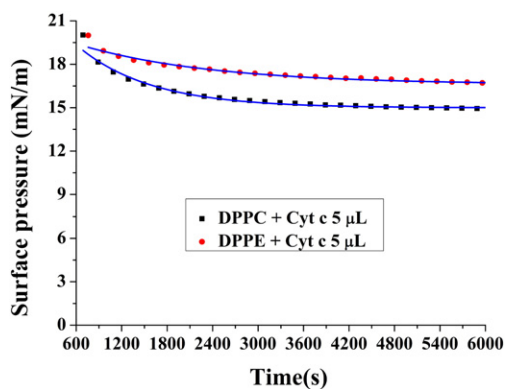


Fig. 7. π -T curves of mixed Cyt c (5 μ L)-DPPC/DPPE monolayer at initial pressure of 20 mN/m. The points represent the corresponding experimental data, theoretical curves (solid lines) calculated from Eq. (4).

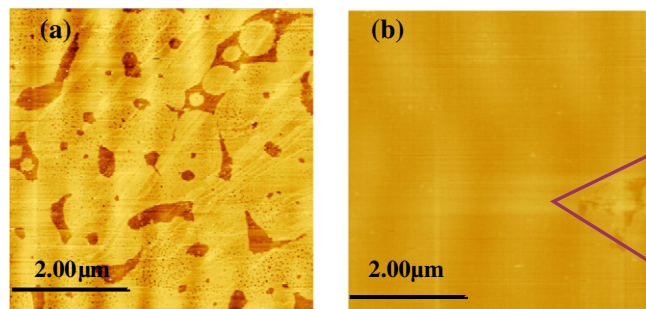


Fig. 8. The AFM images of pure DPPE (a) and pure DPPC (b) monolayer at the scan range $5 \times 5 \mu$ m, transferred on mica at 20 mN/m.

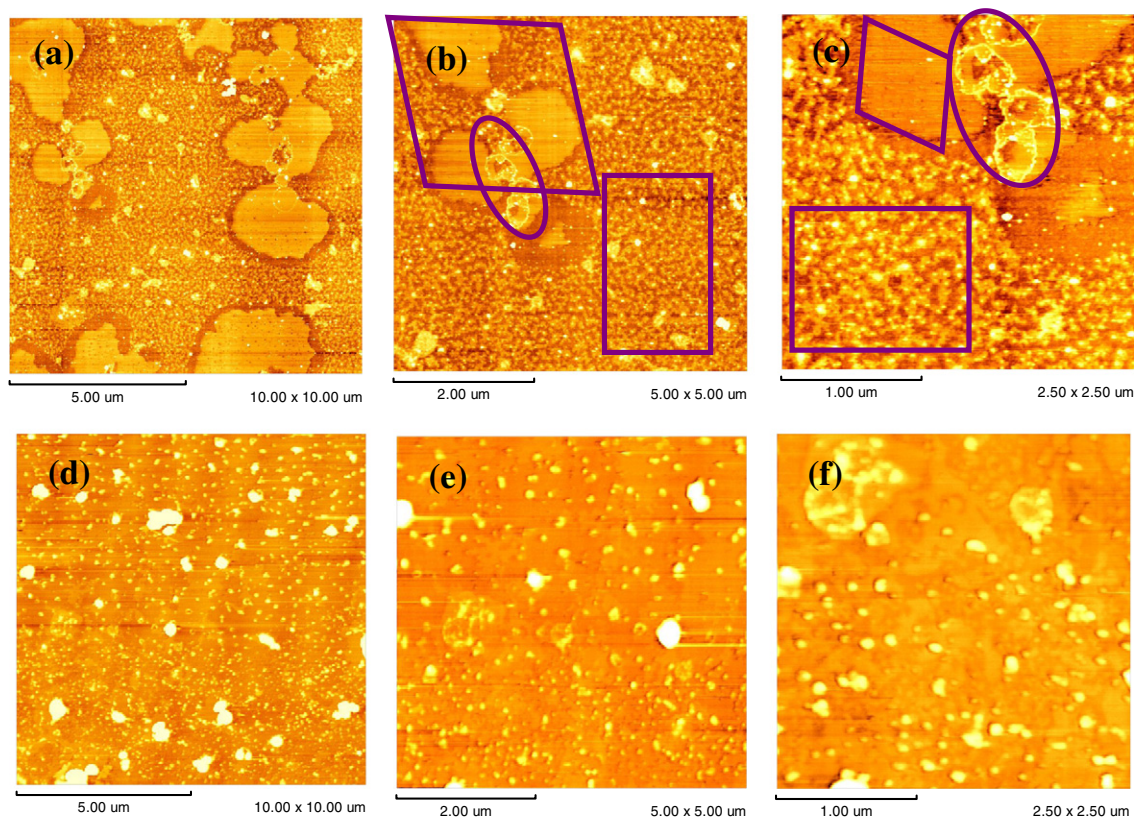


Fig. 9. The AFM images of mixed Cyt c (5 μ L)/DPPE (a–c) and Cyt c (5 μ L)/DPPC (d–f) at different scan ranges, transferred on mica at 20 mN/m.

4. Conclusion

In this paper, we focus on the behavior of different concentrations of Cyt c interacted with DPPC and DPPE at the air–buffer interface. π –A isotherm shows that there is a maximum adsorption quantity of Cyt c on lipid monolayers. Moreover, Cyt c molecules would form aggregations on the surface of lipid monolayers and drag some lipids with them into subphase if the amount of protein exceeds the maximum value (the volume is 2.5 μ L and the concentration is 1×10^{-4} M). Comparing the π –A isotherms of the neutral and negatively charged monolayers, we can also get that the adsorption capacity of Cyt c on the lipid monolayers is DPPS > DPPE > DPPC, which is attributed to their different headgroup structures. The compressibility study reveals that the smaller C_s , the more adsorption of Cyt c on lipid monolayers. AFM images well verify the results of π –A isotherms and C_s – π curves. The π –T curves indicate that it takes more time for protein structure to reorganize after binding to DPPE monolayer than DPPC. The experimental π –A isotherms and π –T curves are well described by a state equation and an order equation,

respectively. All experiments are in very good agreement with the theoretical analysis. These findings successfully serve a possible mechanism to elucidate the interaction of Cyt c with lipid membranes and to control protein molecular quantitative characteristics.

Acknowledgments

The work was supported by the Grant No 21402114 from the National Natural Science Foundation of China; Natural Science Basic Research Plan in Shaanxi Province of China; contract grant number: 2012JQ1002; Fundamental Research Funds for the Central Universities; contract grant number: GK201402010; and Fundamental Research Funds for the Central Universities; contract grant number: GK201504004.

References

- [1] A.-R. Liu, D.-J. Qiao, T. Wakayama, C. Nakamura, J. Miyake, Monolayers, Langmuir–Blodgett films of carbon nanotubes–cytochrome c conjugates and electrochemistry, *Colloids Surf. A Physicochem. Eng. Asp.* 284–285 (2006) 485–489.
- [2] G.B. Khomutov, L.V. Belovolova, V.V. Khanin, E.S. Soldatov, A.S. Trifonov, STM investigation of electron transport features in cytochrome c Langmuir–Blodgett films, *Colloids Surf. A Physicochem. Eng. Asp.* 198–200 (2002) 745–752.
- [3] Ò. Domènech, L. Redondo, M.T. Montero, J. Hernández-Borrell, Specific adsorption of cytochrome c on cardiolipin–glycerophospholipid monolayers and bilayers, *Langmuir* 23 (2007) 5651–5656.
- [4] S. Döner, P. Hildebrandt, F.I. Rosell, A.G. Mauk, M.V. Walter, G. Buse, T. Soulimane, The structural and functional role of lysine residues in the binding domain of cytochrome c in the electron transfer to cytochrome c oxidase, *Eur. J. Biochem.* 261 (1999) 379–391.
- [5] H. Kim, P. Degenaar, Y. Kim, Insertion of a cytochrome c protein into a complex lipid monolayer under an electric field, *J. Phys. Chem. C* 113 (2009) 14377–14380.
- [6] Z. Liu, H. Lin, S. Ye, Q.-Y. Liu, Z.H. Meng, C.-M. Zhang, Y.J. Xia, E. Margoliash, Z.H. Rao, X.-Y. Liu, Remarkably high activities of testicular cytochrome c in destroying reactive oxygen species and in triggering apoptosis, *PNAS* 103 (2006) 8965–8970.
- [7] K. Li, Y.C. Li, J.M. Shelton, J.A. Richardson, E. Spencer, Z.J. Chen, X.D. Wang, R.S. Williams, Cytochrome c deficiency causes embryonic lethality and attenuates stress-induced apoptosis, *Cell* 101 (2000) 389–399.

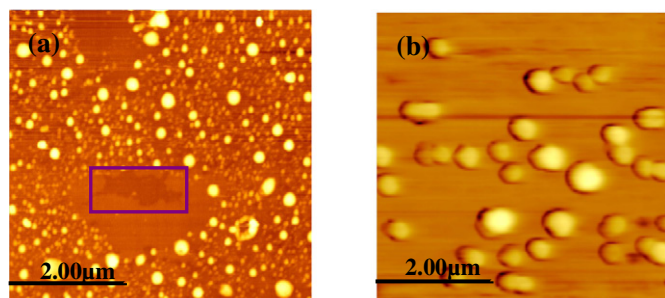


Fig. 10. The AFM images of mixed Cyt c (15 μ L)/DPPE (a) and Cyt c (15 μ L)/DPPC (b) transferred on mica at surface pressure of 20 mN/m.

- [8] Z.Y. Hao, G.S. Duncan, C.-C. Chang, A. Elia, M. Fang, A. Wakeham, H. Okada, T. Calzascia, Y.J. Jang, A. Y.-Ten, W.-C. Yeh, P. Ohashi, X.D. Wang, T.W. Mak, Specific ablation of the apoptotic functions of cytochrome c reveals a differential requirement for cytochrome c and Apaf-1 in apoptosis, *Cell* 121 (2005) 579–591.
- [9] I. Zlatanov, A. Popova, Penetration of lysozyme and cytochrome c in lipid bilayer: fluorescent study, *J. Membr. Biol.* 242 (2011) 95–103.
- [10] J.-H. Yoon, K.-S. Lee, J.E. Yang, M.-S. Won, Y.-B. Shim, Electron transfer kinetics and morphology of cytochrome c at the biomimetic phospholipid layers, *J. Electroanal. Chem.* 644 (2010) 36–43.
- [11] T.J.T. Pinheiro, The interaction of horse heart cytochrome c with phospholipid bilayers: structural and dynamic effects, *Biochimie* 76 (1994) 489–500.
- [12] F. Malatesta, G. Antonini, P. Sarti, M. Brunori, Structure and function of a molecular machine: cytochrome c oxidase, *Biophys. Chem.* 54 (1995) 1–38.
- [13] N. Sanghera, J.T. Pinheiro, Unfolding and refolding of cytochrome c driven by the interaction with lipid micelles, *Protein Sci.* 9 (2000) 1194–1202.
- [14] R.E. Dickerson, T. Takano, D. Eisenberg, O.B. Kallai, L. Samson, A. Cooper, E. Margoliash, Ferricytochrome c general features of the horse and bonito proteins at 2.8 Å resolution, *J. Biol. Chem.* 246 (1971) 1511–1535.
- [15] J.B. Cannon, J.E. Erman, The effect of phospholipid vesicles on the kinetics of reduction of cytochrome c, *Biochem. Biophys. Res. Commun.* 84 (1978) 254–260.
- [16] J. Teissie, Interaction of cytochrome c with phospholipid monolayers. Orientation and penetration of protein as functions of the packing density of film, nature of the phospholipids, and ionic content of the aqueous phase, *Biochemistry* 20 (1981) 1554–1560.
- [17] A.S. Sizov, E.V. Agina, F. Gholamrezaie, V.V. Bruevich, O.V. Borshchev, D.Y. Paraschuk, D.M.D. Leeuw, S.A. Ponomarenko, Oligothiophene-based monolayer field-effect transistors prepared by Langmuir–Blodgett technique, *Appl. Phys. Lett.* 103 (2013) 043310.
- [18] O.I. Kiselyova, O.L. Guryev, A.V. Krivosheev, S.A. Usanov, I.V. Yaminsky, Atomic force microscopy studies of Langmuir–Blodgett films of cytochrome P450sc: hemeprotein aggregation states and interaction with lipids, *Langmuir* 15 (1999) 1353–1359.
- [19] C. Mestres, M. Espina, I. Haro, F. Reig, M.A. Alsina, J.M. García Antón, Miscibility of phosphatidylcholine and sulphatide in monolayers, *Colloid Polym. Sci.* 269 (1991) 1303–1308.
- [20] R. Maget-Dana, The monolayer technique: a potent tool for studying the interfacial properties of antimicrobial and membrane-lytic peptides and their interactions with lipid membranes, *Biochim. Biophys. Acta* 1462 (1999) 109–140.
- [21] P. D.-Latka, A. Dhanabalan, O.N. Oliveira Jr., Modern physicochemical research on Langmuir monolayers, *Adv. Colloid Interf. Sci.* 91 (2001) 221–293.
- [22] Y.-H. Lee, J.-Y. Lin, S. Lee, Adsorption behavior of glucose oxidase on a dipalmitoylphosphatic acid monolayer and the characteristics of the mixed monolayer at air/liquid interfaces, *Langmuir* 23 (2007) 2042–2051.
- [23] G.P. Gorbenko, Y.A. Domanov, Cytochrome c location in phosphatidylcholine/cardiophilin model membranes: resonance energy transfer study, *Biophys. Chem.* 103 (2003) 239–249.
- [24] Z.X. Zeng, D. Li, W.L. Xue, L. Sun, Structural models and surface equation of state for pulmonary surfactant monolayers, *Biophys. Chem.* 131 (2007) 88–95.
- [25] M.-S. Lin, X.-B. Chen, Steven S.-S. Wang, Y. Chang, W.-Y. Chen, Dynamic fluorescence imaging analysis to investigate the cholesterol recruitment in lipid monolayer during the interaction between β -amyloid (1–40) and lipid monolayer, *Colloids Surf. B: Biointerfaces* 74 (2009) 59–66.
- [26] X.K. Chen, Z.S. Huang, W. Hua, H. Castada, H.C. Allen, Reorganization and caging of DPPC, DPPE, DPPG, and DPPS monolayers caused by dimethylsulfoxide observed using Brewster angle microscopy, *Langmuir* 26 (2010) 18902–18908.
- [27] T. Kamilya, P. Pal, G.B. Talapatra, Incorporation of ovalbumin within cationic octadecylamine monolayer and a comparative study with zwitterionic DPPC and anionic stearic acid monolayer, *J. Colloid Interface Sci.* 315 (2007) 464–474.
- [28] A. Aroui, A. Kerth, M. Dathe, A. Blume, The binding of an amphipathic peptide to lipid monolayers at the air/water interface is modulated by the lipid headgroup structure, *Langmuir* 27 (2011) 2811–2818.
- [29] R.G. Sun, C.C. Hao, Y.G. Chang, J. Zhang, C.L. Niu, The thermodynamic properties and morphology observation of sphingosine with DPPC/DPPE monolayer, *Acta Chim. Sin.* 67 (2009) 1808–1814.
- [30] P. Wydro, The interactions between cholesterol and phospholipids located in the inner leaflet of human erythrocytes membrane (DPPE and DPPC) in binary and ternary films—the effect of sodium and calcium ions, *Colloids Surf. B: Biointerfaces* 82 (2011) 209–216.
- [31] A. Thapa, B.C. Vernon, K.D.L. Peña, G. Soliz, H.A. Moreno, G.P. López, E.Y. Chi, Membrane-mediated neuroprotection by curcumin from amyloid- β -peptide-induced toxicity, *Langmuir* 29 (2013) 11713–11723.
- [32] T. Kamilya, P. Pal, M. Mahato, G.B. Talapatra, Effect of salt on the formation of alcohol-dehydrogenase monolayer: a study by the Langmuir–Blodgett technique, *J. Phys. Chem. B* 113 (2009) 5128–5135.
- [33] M. N.-Suárez, N. V.-Romeu, I. Prieto, Behaviour of insulin Langmuir monolayers at the air–water interface under various conditions, *Thin Solid Films* 516 (2008) 8872–8879.